

## On the role of texture and physicochemical characteristics on adsorption capacity of granular activated carbon

N. Pasupulety\*, H. Driss, A. A. Al-Zahrani, M. A. Daous and L. A. Petrov

Chemical & Materials Engineering Department, College of Engineering, King Abdulaziz University, P.O. Box 80204 Jeddah 21589, Saudi Arabia

Received February 5, 2019; Accepted June 1, 2019

Granular activated carbons (GACs) obtained from date's stones were used as adsorbents for the adsorption of phenol, dibenzothiophene (DBT) and 4,6-dimethyl dibenzothiophene (4,6-DMDBT) in solution. The equilibrium adsorption results were correlated with textural and chemical characteristics of GACs. The amount of micropores with pore diameter about 1.289 nm was found high in GAC samples prepared at lower  $ZnCl_2$  ratio ( $R=0.5$ ). These are favorable for phenol and DBT adsorption in solution. SEM analysis revealed pores of elliptical shape for GACs prepared at  $R=0.5$ . GACs with slit-shaped mesopores are beneficial for the adsorption of 4,6-DMDBT in solution. The estimated critical pore diameter was about 0.87 nm for phenol adsorption on GACs. Whereas, the critical pore diameter for adsorption of DBT and 4,6-DBT was about 0.71 and 0.97 nm, respectively, on the studied GACs. GAC samples produced at a lower  $R$  value showed greater amount of total surface functional groups compared to GAC samples prepared at a higher  $R$  value. Hence, the removal performance of phenol was found high on GACs prepared at  $R=0.5$ . However, under identical adsorption conditions, slight hindrance in adsorption of DBT and 4,6-DMDBT was observed on GACs due to the bulkiness of the molecules.

**Keywords:** Granular activated carbon, adsorbent, phenol, dibenzothiophene, 4,6-dimethyl dibenzothiophene

### INTRODUCTION

Activated carbon (AC) is successfully prepared from different agricultural wastes such as apricot stones, date fruit stones, nutshells, plum kernels, and rice husks [1-9]. It is also produced from various municipal wastes such as PET waste, sewage sludge and discarded tires [10-14]. It is well known that porous materials like AC have high adsorption capacity for a variety of liquid and gas adsorbates [15]. AC is also widely used in catalysis [16,17], food, beverage and pharmaceutical industries [18,19]. The surface chemistry of AC plays a key role in adsorption mechanisms and behaviors [20,21].

Dry date's stones contain 5-10% moisture, 6-7% proteins, 7-10% oil, 1-2% ash, 10-20% crude fibers and 55-65% carbohydrates [22]. They have the lowest lignin content, the highest cellulose and hemicellulose contents compared with almond shells, pecan shells and walnut shells [4]. The surface chemistry of GAC depends on pretreatment conditions such as acid concentration (HCl), activation temperature, and activation time [23]. Therefore, the physicochemical characteristics of GAC samples prepared under different conditions were investigated in this study. GAC samples produced with different chemical activator-to-date's stones weight ratio ( $R$ ), carbonization temperature ( $T_c$ ) and carbonization time ( $t_c$ ) were employed in phenol, DBT and DMDBT adsorption

experiments. Date's stones impregnation with  $ZnCl_2$  causes degradation of the cellulosic material upon carbonization. The dehydration and degradation of the cellulosic material result in charring, aromatization of the carbon skeleton and creation of the pore structure [24].  $ZnCl_2$  selectively strips H and O away from date's stones as  $H_2O$  and  $H_2$  rather than hydrocarbons, CO or  $CO_2$  [25].

In this paper, BET surface area and SEM analysis was used to determine the textural parameters of lab prepared GAC samples. Surface functional groups were determined by using Boehm titrations and XPS. The equilibrium adsorption data of phenol, DBT and DMDBT were fitted to Langmuir isotherm equation. The possible correlation between the textural properties and phenol, DBT and DMDBT removal performance of the GAC samples are discussed.

### EXPERIMENTAL

The detailed preparation of GACs and the carbonization process are reported elsewhere [26]. The carbonization process was done at two different temperatures  $T_c = 600$  or  $700$  °C with duration of 1 and 3 h ( $t_c$ ). The samples prepared at  $T_c = 600$  °C,  $R=0.5$  and  $t_c = 1$  and 3 h are labeled as GAC 1 and 2, respectively. The samples prepared at  $T_c = 700$  °C,  $R=0.5$  and  $t_c = 1$  and 3 h are labeled as GAC 3 and 4, respectively. The samples prepared at  $T_c = 600$  °C,  $R=2$  and  $t_c = 1$  and 3 h are labeled as GAC 5 and 6, respectively. The samples

\* To whom all correspondence should be sent:

E-mail: pasupulety@gmail.com;  
nsampathra@kau.edu.sa

*N. Pasupulety et al.: On the role of texture and physicochemical characteristics on adsorption capacity of granular ...*  
 prepared at  $T_c = 700\text{ }^\circ\text{C}$ ,  $R=2$ ,  $t_c = 1$  and  $3\text{ h}$  are labeled as GAC 7 and 8, respectively.

### Adsorption measurements

#### Characterization

BET surface area and pore size measurements were performed on a NOVA 2200e instrument (Quntachrome). Multipoint BET surface area, pore size and total pore volume measurements were done using NOVWIN software provided with the equipment. Sample morphology was determined by using FE-SEM, equipped with ETD and VC detectors. XPS results of GAC samples were collected on a SPECS GmbH system equipped with Mg  $K\alpha$  1253.6 eV X-ray source. The reported binding energy values are based on C 1s 285.0 eV. The surface acid-base groups of the produced GAC samples were determined by the Boehm titration method [15, 16]. One gram of GAC sample each was placed in  $50\text{ cm}^3$  of 0.1 N solutions of the following reagents: sodium hydroxide, sodium carbonate, sodium bicarbonate and hydrochloric acid. The vials were sealed and shaken for 24 h at room temperature ( $25\text{ }^\circ\text{C}$ ). Later, each of these solutions was filtered and  $5\text{ cm}^3$  of filtrate was titrated with HCl (0.1 N) or NaOH (0.1 N), respectively. The number of acidic sites was determined under the assumption that NaOH neutralizes carboxylic, lactonic and phenolic groups; sodium carbonate neutralizes carboxylic and phenolic groups and sodium bicarbonate neutralizes only carboxylic acid groups. The number of the basic sites was calculated from the amount of hydrochloric acid that reacted with the carbon surface.

Equilibrium adsorption studies of phenol were conducted by using  $25\text{ cm}^3$  of phenol-water solutions with concentrations between 10 and 150 mg/l using 0.1 g of GAC sample with an average particle size of 1.50 mm. The adsorption measurements of the control sample were carried out at temperature of  $25\text{ }^\circ\text{C}$  under continuous shaking for 24 and 48 h. The initial and final concentration of phenol was determined using a Genysis10 UV/Vis spectrophotometer calibrated at  $\lambda_{\text{max}}=268\text{ nm}$ .

DBT and 4,6-DMDBT decane solutions with concentration between 10 and 200 mg/l were used for equilibrium adsorption studies. Each, 0.4 g of GAC sample with an average particle size of 1.0 mm was charged into a conical flask containing the above solutions and adsorption studies were conducted at room temperature of  $25\text{ }^\circ\text{C}$  under continuous stirring. The concentrations of DBT and 4,6-DMDBT before and after the adsorption were determined by using Shimadzu GC equipped with Rxi-5ms capillary column fitted to FID. The collected adsorption data were fitted to a Langmuir isotherm described by the equation below:

$$q_e = q_m \frac{K_L C_e}{1 + K_L C_e}$$

where,  $q_m$  is the amount of solute (phenol, DBT and DMDBT) adsorbed in  $\text{mg g}^{-1}$  of dry GAC,  $C_e$  is the equilibrium concentration of the phenol, DBT and 4,6-DMDBT in solution in  $\text{mg l}^{-1}$ .  $K_L$  is Langmuir constant [27].

## RESULTS AND DISCUSSIONS

### Nitrogen adsorption isotherms

Nitrogen adsorption isotherms of GAC samples are shown in Fig. 1.

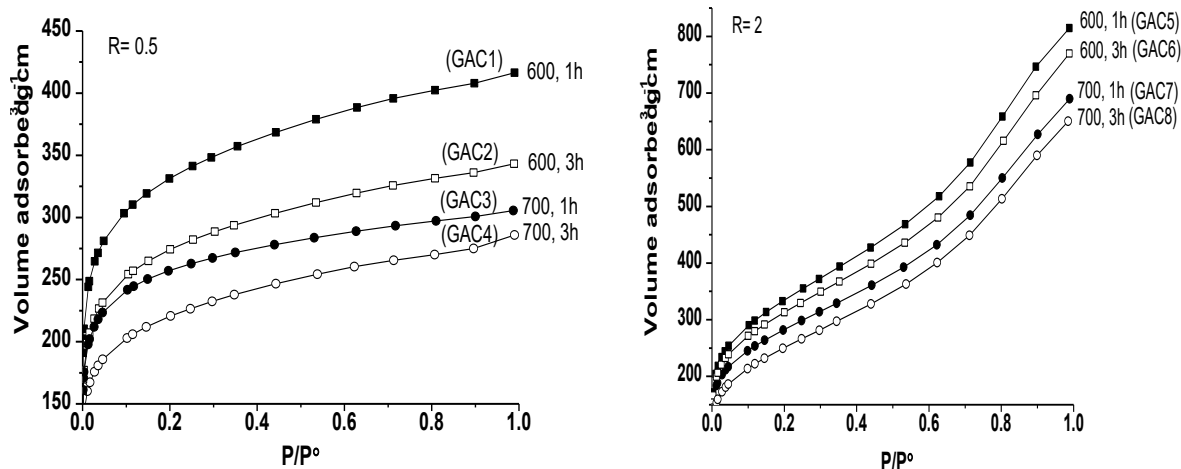


**Fig. 1.** Nitrogen adsorption isotherms of GAC samples prepared at  $R=0.5$  and  $2$ .

**Table 1.** Nitrogen adsorption parameters of GAC samples.

Sample	BET surface area $\text{m}^2 \text{g}^{-1}$	* Total SA $\text{m}^2 \text{g}^{-1}$	* Micropore area $\text{m}^2 \text{g}^{-1}$ ( $\text{dp} < 2 \text{nm}$ )	* $V_t$ $\text{cm}^3 \text{g}^{-1}$	* $V_{\text{meso}}$ $\text{cm}^3 \text{g}^{-1}$	* $V_{\text{micro}}$ $\text{cm}^3 \text{g}^{-1}$	* $d_p \text{ MAX}$ nm	* $d_p \text{ nm}$
GAC1	1212.4	1505	1210	0.619	0.200	0.419	1.289	1.289
GAC2	998.5	1279	1049	0.510	0.164	0.346	1.328	1.289
GAC3	802.0	1030	835	0.421	0.149	0.272	1.289	1.289
GAC4	951.0	1300	1143	0.456	0.101	0.355	1.276	1.289
GAC5	1172.0	1207	482	1.171	0.972	0.199	1.646	1.686
GAC6	1106.8	1159	486	1.095	0.894	0.201	1.7	1.487
GAC7	990.8	1081	492	0.984	0.806	0.178	1.6	1.646
GAC8	984.9	1075	472	0.971	0.797	0.174	1.48	1.567

$V_t$  = total pore volume;  $V_{\text{mic}}$  = micropores ( $< 2 \text{ nm}$ );  $V_{\text{meso}}$  = mesopores ( $2\text{-}50 \text{ nm}$ );  $d_p \text{ MAX}$  = pore diameter maxima in nm;  $d_p$  = pore diameter; \* = NLDFT cylindrical pore model.

Pore size distribution data were obtained by using nonlinear density function theory (NLDFT) adopting the cylindrical pore model and are presented in Table 1. Predominant micropores were observed over mesopores in GAC samples produced at  $R=0.5$ , whereas systematic development of mesoporosity was observed in GAC samples prepared at  $R=2$ . Further, an increase in the activation temperature ( $T_c$ ) decreased the micropore volume in the studied GAC samples. The total pore volume and pore diameter ( $d_p$ ) were increased with the increase in  $R$  value (Table 1). The BET surface area was found to be high in  $600 \text{ }^\circ\text{C}$ -activated samples, whereas the BET surface area of GAC samples activated at  $700 \text{ }^\circ\text{C}$  was lower at a given  $R$  value. This decrease in the surface area is associated with pore collapse most probably caused by the heat treatment [29]. The surface area and pore size distribution results suggest that pores were developed with different sizes during the activation of the prepared GAC samples.

#### SEM studies

Textural properties of synthesized GAC samples were studied through SEM analysis. The micrographs at  $R=0.5$  and  $2$  for  $T_c = 600$  or  $700 \text{ }^\circ\text{C}$ , respectively, are presented in Fig. 2. At  $R=0.5$ , the influence of  $T_c$  and  $t_c$  on the textural properties of GAC samples is shown in Fig. 2a to c. Formation of pores with elliptical shape with pore diameter about  $2 \text{ } \mu\text{m}$  was observed for  $T_c = 600$  or  $700 \text{ }^\circ\text{C}$  (Fig. 2a, b) at  $t_c = 1 \text{ h}$ , whereas, the elliptical-shaped pores with larger size ( $4 \text{ } \mu\text{m}$ ) were observed at  $t_c = 3 \text{ h}$  and  $T_c = 700 \text{ }^\circ\text{C}$  (Fig. 2c, GAC4). The results suggest that pore-widening process took place with the increase in  $T_c$  from  $600$  to  $700 \text{ }^\circ\text{C}$  and with increase in  $t_c$  from  $1 \text{ h}$  to  $3 \text{ h}$ .

Slit-like pores with the size of opening between  $10$  and  $13 \text{ } \mu\text{m}$  and width between  $3$  and  $7 \text{ } \mu\text{m}$  were observed at  $R=2$  (Fig. 4, GAC8). Further, the widening process transformed elliptical-shaped pores to slit-shaped pores for the GAC samples

produced at  $R=2$  and  $T_c=700 \text{ }^\circ\text{C}$ . Pores development in the GAC samples was associated with the removal of  $\text{ZnCl}_2$  residues and other impurities such as  $\text{ZnO}$  during the washing and activation process. In addition, only  $16\%$  of  $\text{ZnCl}_2$  was recovered after the activation and washing process for GAC4 sample which suggests that the removal of  $\text{ZnCl}_2$  is intensified by means of evaporation at heat treatment of  $700 \text{ }^\circ\text{C}$  for  $3 \text{ h}$  at  $R=0.5$  [26].

At  $R=2$ , smooth melt structure was observed in the images and the presence of this melt would reduce the surface pores area of the GAC samples. Under identical  $T_c$  and  $t_c$  the removal of  $\text{ZnCl}_2$  and  $\text{ZnO}$  impurities was intensified in samples produced at  $R=0.5$  compared to samples prepared at  $R=2$  [26]. Activation of GACs above  $700 \text{ }^\circ\text{C}$  resulted in caking and agglomeration on the char structure and thus produced chars with an intact external surface [30]. The SEM images are in agreement with pore size distribution studies, wherein slit-like mesopores were observed for GAC samples produced at  $R=2$ .

#### Boehm titration results

Acid and base surface functional groups of the prepared GAC samples were accessed through Boehm titrations and the data are presented in Table 2. Principally, three types of acid functional groups are known in activated carbons such as carboxylic, lactonic and phenolic groups. Similar acid functional groups were observed in the studied GAC samples after different activation processes. Nevertheless, GAC samples produced at lower  $R$  values showed a greater amount of total surface functional groups per microporous surface area compared to GAC samples prepared at higher  $R$  values. Further, acid groups were predominant over base groups in the studied GAC samples. The result suggests that all the GAC samples are acidic in character.

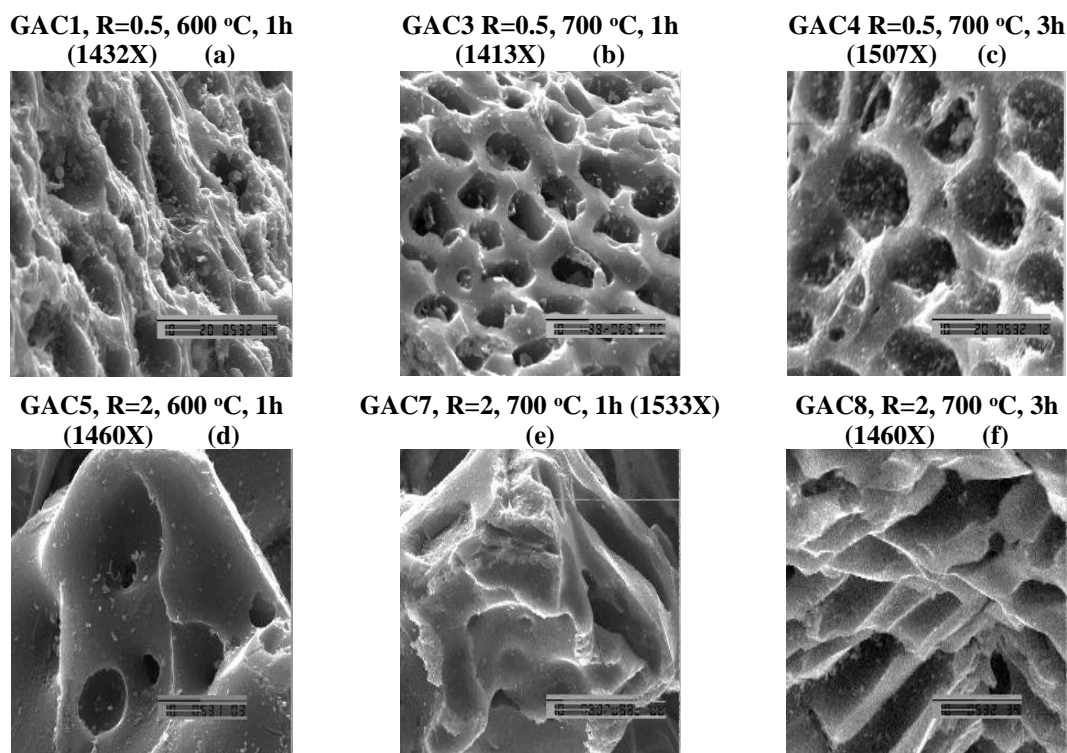


Fig. 2. SEM micrographs of the GAC samples prepared by different activation processes

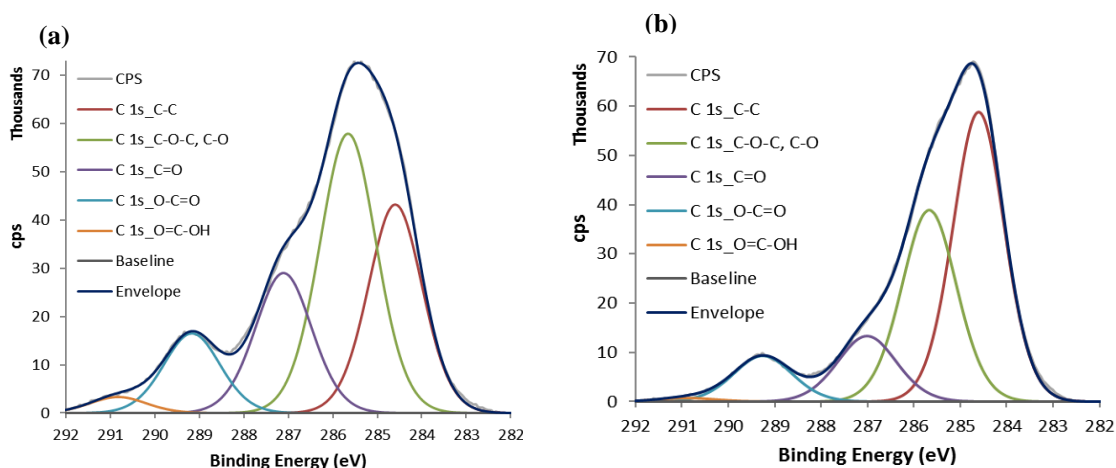


Fig. 3. XPS analysis of (a) GAC4 and (b) GAC8 samples.

### XPS results

C1s XPS results of GAC4 and GAC8 samples are presented in Fig. 3.

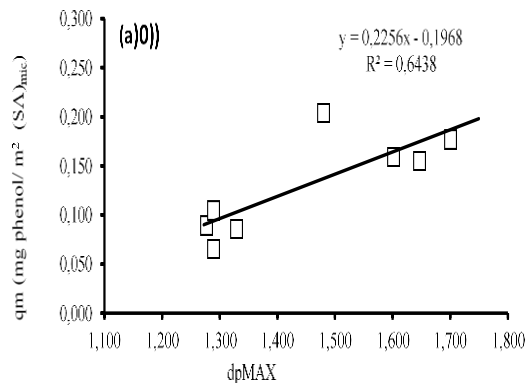
These samples show a broad pattern in the binding energy region of 282-292 eV. The Shirley deconvolution yielded five chemically-shifted signals centered at 284.6, 285.8, 287.1, 289.3 and 290.9 eV, respectively. The signal at 284.6 eV was ascribed to  $Sp^3$  carbon present in GAC.

Four more carbon-related components at 285.8, 287.1, 289.3 and 290.9 eV were assigned to -C-O, carbonyl (-C=O), carboxylate (-O-C=O) and

carboxyl (-COOH) functionalities, respectively. Presence of  $sp^3$  carbon suggests the existence of unoxidized domains in the prepared samples. These results were in agreement with Boehm titrations wherein acid-base functional groups were detected. It is clear from the XPS results that transformation of unoxidized domains to oxidized functional groups was intensified at a lower R value ( $R=0.5$ ) compared to the higher R value ( $R=2.0$ ) during the activation at 700 °C for 3 h. It is associated with removal of  $ZnCl_2$  and other zinc impurities from the samples during the activation process.

### Phenol removal by GAC samples

GACs used for phenol adsorption measurements had an average grain size of 1.50 mm. Surface diffusivity and faster adsorption rate can be attributed to the lower internal mass transfer resistance of the adsorbent due to its large pore size



[31]. Phenol molecule size was reported between 0.46 and 0.55 nm [32]. Critical pore diameter (dp critical) for phenol adsorption on GACs was estimated by plotting the graph between dp MAX and Langmuir adsorption capacity (qm) per micropore surface area.

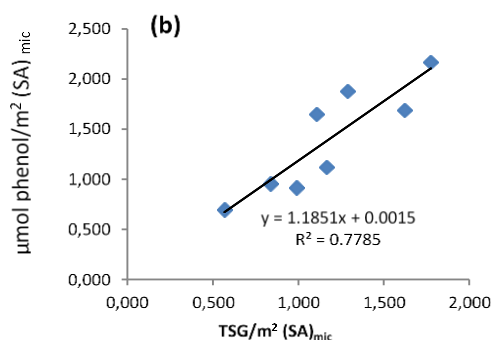


**Fig. 4** (a) Critical pore diameter of GACs in phenol adsorption; (b) TSG *versus* phenol adsorption capacity of GACs.

Solving the linear equation in Fig. 4a led to the dp critical value of 0.87 nm. The estimated dp critical value is much higher than the phenol molecule size. In addition, the micropore volume was found to be high in GACs prepared at R=0.5 compared to R=2 (Table 1). For GAC1 to 4, the pore diameter was about 1.289 nm and the amount of these pores were found high in these samples compared to GAC5 to 8. Hence, greater adsorption capacity for phenol was observed.

Fig. 4b shows the correlation between phenol adsorption capacity and total surface functional groups. Linear regression was used to calculate the correlation coefficient ( $R^2$ ). The obtained  $R^2$  value was about 0.778, which suggests that adsorbent surface functional groups are vital for the adsorption of phenol in solution. The Boehm titration results in Table 2 clearly demonstrate that development of surface function groups was facile at R=0.5 compared to R=2.0. Moreover, phenol is a weak acid and the surface with a greater number of basic functional groups can adsorb a greater amount of phenol than other surfaces with a smaller number of basic functional groups. Hence, GAC2 and GAC4 samples with adequate surface basicity with greater total surface functional groups (TSG) have exhibited greater phenol adsorption capacity.

### DBT and 4,6-DMDBT removal by GAC samples

GACs used for sulfur adsorption measurements had an average grain size of 1.0 mm. DBT and 4,6-

DMDBT molecule size was reported approximately in the range of 0.70 to 0.80 nm [33].

The estimated critical pore diameter for DBT and 4,6-DMDBT was about 0.71 and 0.97 nm, respectively, from the linear regression equations in Fig. 5a. It is clear from Tables 1 and 2 data that DBT adsorption is high on GAC1 to 4 samples which have a greater amount of micropores with pore diameter of 1.289 nm. Further, the graph between TSG of GACs *versus* sulfur adsorption data in Fig. 5b yielded  $R^2$  value of 0.70 which is less than phenol  $R^2$  value. The result reveals that there is a hindrance for DBT adsorption on GACs due to its bulkiness. Further, the dp critical value for DBT adsorption on GACs (0.71 nm) is close to the molecular size of DBT which also indicates strain in its adsorption. Hence, the adsorption tendency for DBT is less than for phenol on GACs under identical adsorption conditions. In case of 4,6-DMDBT the estimated critical pore diameter was about 0.97 nm (Fig. 5a, triangles). The plot between TSG of GACs *versus* sulfur adsorption capacity in Fig. 5c produced  $R^2$  value of 0.69, which is slightly less than DBT  $R^2$  value. It is obvious from the results that the methyl groups present on DMDBT slightly increased the adsorption resistance on GACs (Table 2).

Therefore, samples with a greater number of mesopores (GAC5 to 8) showed greater adsorption tendency for 4,6-DMDBT. Furthermore, SEM analysis revealed ordered elliptical-shaped pores for GACs prepared at R=0.5 which are favorable

N. Pasupulety et al.: On the role of texture and physicochemical characteristics on adsorption capacity of granular ... for phenol and DBT adsorption. On the other hand, GAC5 to 8 seem to be advantageous for 4,6-DMDBT adsorption in solution.

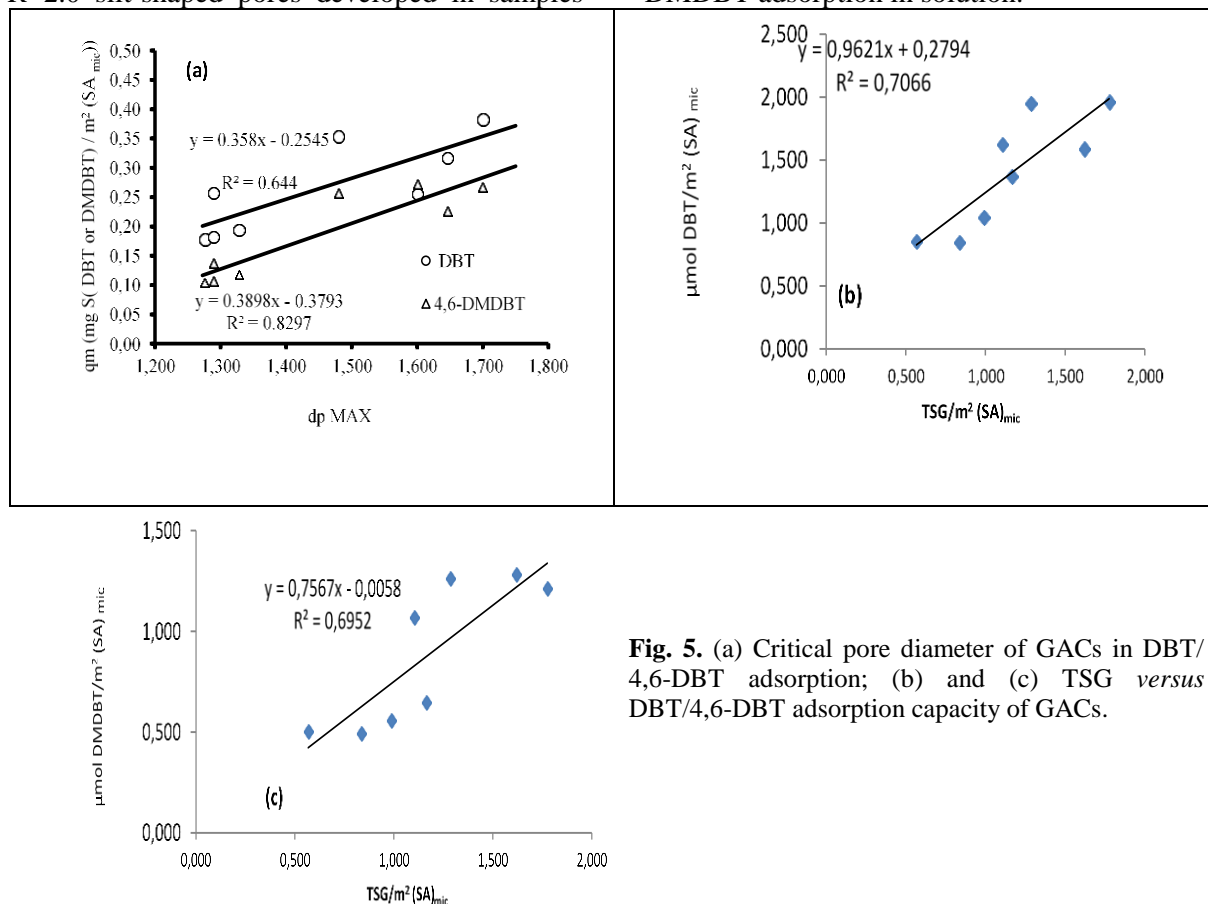


**Fig. 5.** (a) Critical pore diameter of GACs in DBT/ 4,6-DBT adsorption; (b) and (c) TSG versus DBT/4,6-DBT adsorption capacity of GACs.

## CONCLUSIONS

Elliptical-shaped pores were developed in GACs prepared at R=0.5. GACs prepared at R=0.5 have a greater amount of micropores favorable for adsorption of phenol and DBT in solution. Slit-shaped pores were developed in GACs obtained at R=2.0. These samples were rich in mesopores beneficial for 4,6-DMDBT adsorption in solution. GAC samples produced at a lower R value showed a greater amount of total surface functional groups compared to GAC samples prepared at a higher R

value. Hence, the removal performance of phenol was found high on GACs prepared at R=0.5. However, slight hindrance in adsorption of DBT and 4,6-DMDBT was observed on GACs due to the bulkiness of the molecules.

**Acknowledgements:** This work was supported by the Deanship of Scientific Research (DSR), King Abdulaziz University, Jeddah, under grant no.(D-090-135-1439). The authors, therefore, gratefully acknowledge the DSR technical and financial support.

**Table 2.** Boehm titration results and Langmuir adsorption capacity of GAC samples.

Sample	Carboxylic mM g <sup>-1</sup>	Lactonic mM g <sup>-1</sup>	Phenolic mM g <sup>-1</sup>	Base mM g <sup>-1</sup>	Total surface groups (TSG)	q <sub>m</sub> (mg g <sup>-1</sup> ) phenol	q <sub>m</sub> (mg g <sup>-1</sup> ) DBT	q <sub>m</sub> (mg g <sup>-1</sup> ) 4,6- DMDBT
GAC1	0.327	0.283	0.083	0.099	0.792	79.72	38.01	19.59
GAC2	0.407	0.284	0.110	0.253	1.054	104.80	35.01	18.64
GAC3	0.219	0.273	0.233	0.234	0.959	87.88	36.56	17.32

GAC4	0.357	0.271	0.048	0.299	0.975	103.00	35.00	18.06
GAC5	0.179	0.282	0.195	0.066	0.722	74.93	26.87	16.48
GAC6	0.260	0.298	0.013	0.208	0.779	85.99	33.31	19.61
GAC7	0.356	0.282	0.022	0.199	0.859	78.35	21.89	20.19
GAC8	0.289	0.252	0.151	0.219	0.911	96.57	29.63	18.32

#### REFERENCES

1. K. Gergova, S. Eser, *Carbon*, **34**, 879 (1996).
2. C.A. Philip, B.S. Girgis, *J. Chem. Technol. Biotechnol.*, **67**, 248 (1996).
3. A.A.M. Daifullah, B.S. Girgis, *Water Res.*, **32**, 1169 (1998).
4. C.A. Toles, W.E. Marshall, M.M. Johns, *J. Chem. Technol. Biotechnol.*, **72**, 255 (1998).
5. C.A. Toles, W.E. Marshall, M.M. Johns, *Carbon*, **37**, 1207 (1999).
6. M. Ahmedna, W.E. Marshall, R.M. Rao, *Bioresour. Technol.*, **71**, 113 (2000).
7. R.S. Juang, F.C. Wu, R.L. Tseng, *J. Colloid Interface Sci.*, **227**, 437 (2000).
8. Y.L. Diao, W.P. Walawender, L.T. Fan, *Bioresour. Technol.*, **81**, 45 (2002).
9. L.J. Kennedy, J.J. Vijaya, G. Sekaran, *Ind. Eng. Chem. Res.*, **43**, 1832 (2004).
10. S. Nagano, H. T. Tamon, T. Adzumi, K. Nakagawa, T. Suzuki, *Carbon*, **38**, 915 (2000).
11. K. Nakagawa, T. Sugiyama, S.R. Mukai, H. Tamon, Y. Shira, W. Tanthapanichakoon, *J. Chem. Eng. Jpn.*, **37**, 889 (2004).
12. F. Rozada, M. Otero, A. Moran, A.I. Garcia, *J. Hazard. Mater.*, **124**, 181 (2005).
13. V. Boonamnuyvitaya, S. Sae-ung, W. Tanthapanichakoon, *Sep. Purif. Technol.*, **42**, 159 (2005).
14. F.S. Zhang, J.O. Nriagu, H. Itoh, *Water Res.*, **39**, 389 (2005).
15. B.S. Girgis, A.A. Attia, N.A. Fathy, *Colloids Surf. A.*, **299**, 79 (2007).
16. J.D. Webb, S. MacQuarrie, K. McEleney, C.M. Crudden, *J. Catal.*, **252**, 97 (2007).
17. X.L. Tang, J.M. Hao, H.H. Yi, J.H. Li, *Catal. Today*, **126**, 406 (2007).
18. H. Marsh, in: *Activated Carbon Compendium: A collection of papers from the journal Carbon 1996–2000*. Elsevier, Amsterdam, 2001.
19. C. Moreno-Castilla, M.A. Alvarez-Merino, M.V. Lopez-Ramon, J. Rivera-Utrilla, *Langmuir*, **20**, 8142 (2004).
20. M. F. R. Pereira, S. F. Soares, J. J. M. Orfao, J. L. Figueiredo, *Carbon*, **41**, 811 (2003).
21. C. Moreno-Castilla, *Carbon*, **42**, 83 (2004).
22. B.S. Girgis, A.N.A. El-Hendawy, *Microporous Mesoporous Mater.*, **52**, 105 (2002).
23. Y. A. Alhamed, *J. Hazard. Mater.*, **170**, 763 (2009).
24. M. Smisek, S. Cerny, in: *Active Carbon: Manufacture, Properties and Applications*, Elsevier, Amsterdam, 1970.
25. Q.R. Qian, M. Machida, H. Tatsumoto, *Bioresour. Technol.*, **98**, 353 (2007).
26. Y. A. Alhamed, *Bulg. Chem. Commun.*, **40**, 26 (2008).
27. R. C. Bansal, M. Goyal, in: *Activated Carbon Adsorption*, Taylor & Francis Group, London, 2005.
28. A.M. Warhurst, G.D. Fowler, G.L. McConnachie, S.J.T. Pollard, *Carbon*, **35**, 1039 (1997).
29. M.A. Al-Omar, E.A. El-Sharkawy, *Environ. Technol.*, **28**, 443 (2007).
30. A. Ahmadpour, D.D. Do, *Carbon*, **35**, 1723 (1997).
31. S. Haji, C. Erkey, *Ind. Eng. Chem. Res.*, **42**, 6933 (2003).
32. L.-G. Ewa, *Adsorption*, **22**, 599 (2016).
33. Z. Wenwu, L. Meifang, Z. Yasong, W. Qiang, Z. Qing, *Energy & Fuels*, **31**, 7445 (2017).